Heterobimetallic Indenyl Complexes. Mechanism of Cyclotrimerization of Dimethyl Acetylenedicarboxylate (DMAD) Catalyzed by *trans*-[Cr(CO)$_3$(Heptamethylindenyl)Rh(CO)$_2$][†]

Laura Mantovani, Alberto Ceccon,* Alessandro Gambaro, and Saverio Santi

Dipartimento di Chimica Fisica, Università di Padova, Via Loredan 2, 35131 Padova, Italy

Paolo Ganis

Dipartimento di Chimica, Università di Napoli, Via Mezzocannone 4, 80134 Napoli, Italy

Alfonso Venzo

CNR, Centro di Studio sugli Stati Molecolari, Radicalici ed Eccitati, Via Loredan 2, 35131 Padova, Italy

Received October 24, 1996[⊗]

The complex *trans*-[Cr(CO)$_3$(heptamethylindenyl)Rh(CO)$_2$] (**II**) is a very efficient catalyst precursor in the cyclotrimerization reaction of dimethyl acetylenedicarboxylate (DMAD) to hexacarbomethoxybenzene. The formation of the "true" catalyst, likely to be the complex *trans*-[Cr(CO)$_3$−Ind*−Rh(DMAD)$_2$], is the slow step of the reaction and takes place during the induction period, the length of which is temperature dependent. After total consumption of the monomer two organometallic complexes were isolated from the inorganic residue, *viz.*, the catalyst precursor **II** and the complex *trans*-[Cr(CO)$_3$−Ind*−Rh(CO)(FADE)] (**III**; FADE = fumaric acid dimethyl ester), which turns out to be active in the trimerization reaction as **II**. The hydrogenation of DMAD to FADE is probably occurring *via* C−H bond activation of the solvent cyclohexane.

Introduction

The use of [(η^5-cyclopentadienyl)RhL$_2$]-like complexes as catalysts for cyclotrimerization of alkynes was studied some years ago,[1] in particular for L$_2$ = 1,5-cyclooctadiene (COD).[1a] The rates of cyclotrimerization appear to vary with the nature of the ancillary ligand L, and one of the various pathways proposed implies that L remains bound to the rhodium atom throughout the catalytic cycle. The cyclotrimerization reaction catalyzed by (η-Ind)Rh(COD) is approximately 10 times faster than the corresponding reaction promoted by (η-Cp)Rh(COD),[1a,b] and the enhanced reactivity was attributed to a greater flexibility of the indenyl ligand to coordinate rhodium in different bonding modes.[2]

Recent work on bimetallic indenyl complexes has demonstrated that the catalytic activity of (η-indenyl)-RhL$_2$ complexes increases dramatically (from 7 to 70 times depending on the nature of the monomer and the reaction conditions) if the benzene ring of the indenyl ligand is coordinated with Cr(CO)$_3$ in a transoid arrangement ("extra indenyl effect").[3] This effect is absent when the two metal groups are situated in a cisoid arrangement.[4] Further improvement in the trimerization reaction of methyl propiolate (MP) and dimethyl acetylenedicarboxylate (DMAD) was achieved when the heptamethylindenyl (Ind*) species was used as ligand;[3b] in fact, the use of the complex *trans*-[Cr(CO)$_3$−Ind*−Rh(COD)] (**I**) as catalyst allowed the almost quantitative conversion of the monomer MP to substituted benzenes with no reduction of the rate throughout the entire reaction, whereas the conversion promoted by the non-methylated catalyst was only 80%. Unlike the (cyclopentadienyl)Rh(CO)$_2$ complexes that have been shown not to follow simple kinetics and to be converted into some kinetically inactive species during the reaction,[1a] the complex *trans*-[Cr(CO)$_3$−Ind*−Rh(CO)$_2$] (**II**) maintains its catalytic efficiency up to the almost quantitative conversion of the monomer.[3b]

We report herein a mechanistic study of the cyclotrimerization reaction of dimethyl acetylenedicarboxylate carried out by using **II** as a catalyst precursor. Easy spectroscopic recognition of **II** made it possible to follow its fate during the reaction; in addition, it was possible

[†] Taken in part from the Ph.D. thesis of L.M., Università di Padova, 1996.

[⊗] Abstract published in *Advance ACS Abstracts,* March 15, 1997.

(1) (a) Abdulla, K.; Booth, B. L.; Stacey, C. *J. Organomet. Chem.* **1985**, *293*, 103. (b) Borrini, A.; Diversi, P.; Ingrosso, G.; Lucherini, A.; Serra, G. *J. Mol. Catal.* **1985**, *30*, 181 and references therein. (c) Collman, J. O.; Kang, J. W.; Little, W. F.; Sullivan, M. F. *Inorg. Chem.* **1968**, *7*, 1298.

(2) (a) White, C.; Mawby, R. J. *Inorg. Chim. Acta* **1970**, *4*, 261. (b) White, C.; Mawby, R. J.; Hart-Davis, A. J. *Inorg. Chim. Acta* **1970**, *4*, 441. (c) Jones, D. J.; Mawby, R. J. *Inorg. Chim. Acta* **1971**, *6*, 157. (d) Turaki, N. N.; Huggins, J. M. *Inorg. Chem.* **1988**, *27*, 424. (e) Caddy, P.; Green, M.; O'Brien, E.; Smart, L. E.; Woodward, P. *J. Chem. Soc., Dalton Trans.*, **1980**, 962; *Angew. Chem., Int. Ed. Engl.* **1977**, *16*, 648. (f) Rerek, M. E.; Basolo, F. *J. Am. Chem. Soc.* **1984**, *106*, 5908. (g) Ji, L.-N.; Basolo, F. *Organometallics* **1984**, *3*, 740. (h) Hart-Davis, A. J.; Mawby, R. J. *J. Chem. Soc. A* **1969**, 2403. (i) Marder, T. B.; Williams, I. D. *J. Chem. Soc., Chem. Commun.* **1987**, 1478. (j) Kakkar, A. K.; Taylor, N. J.; Marder, T. B. *Organometallics* **1989**, *8*, 1765. (k) Estiag-Hosseini, H.; Nixon, J. F. *J. Less-Common Met.* **1987**, *61*, 107. (l) Brown, D. A.; Fitzpatrick, N. J.; Glass, W. K.; Hamed, H. A.; Cunningham, D.; McArdle, P. *J. Organomet. Chem.* **1993**, *455*, 167.

(3) (a) Ceccon, A.; Gambaro, A.; Santi, S.; Venzo, A. *J. Mol. Catal.* **1991**, *69*, L1−L6. (b) Bonifaci, C.; Ceccon, A.; Gambaro, A.; Ganis, P.; Mantovani, L.; Santi, S.; Venzo, A. *J. Organomet. Chem.* **1994**, *475*, 267.

(4) Bonifaci, C. Ph.D. Thesis, University of Padova.

S0276-7333(96)00901-6 CCC: $14.00

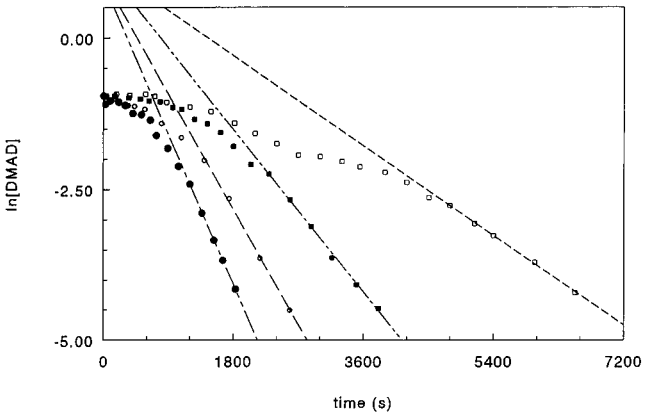

Figure 1. Plots of ln[DMAD] *vs* time for the cyclotrimerization reaction of DMAD catalyzed by *trans*-[$Cr(CO)_3$−Ind*−$Rh(CO)_2$] in cyclohexane ([DMAD]$_0$ = 0.387 M, [DMAD]$_0$/[cat.] = 1000) (●), T = 50 °C; (○) T = 42 °C; (■) T = 34 °C; (□) T = 25 °C.

Table 1. k_{obsd} Values (s^{-1}) for the Cyclotrimerization Reaction of DMAD Catalyzed by *trans*-[$Cr(CO)_3$−Ind*−$Rh(CO)_2$] (II), *trans*-[$Cr(CO)_3$−Ind*−Rh(CO)(FADE)] (III), and *trans*-[$Cr(CO)_3$−Ind*−Rh(CO)(MADE)] (IV) [DMAD]$_0$ = 0.387 M)

catalyst	10^4[cat.], M	[DMAD]$_0$/[cat.]	T, °C	10^3k_{obsd}, s^{-1}
II	3.8	1000	25	0.82
II	3.8	1000	34	1.5
II	3.8	1000	42	2.1
II	3.8	1000	50	2.8
II	1.9	2000	50	1.9
II	1.3	3000	50	1.5
III	3.8	1000	50	3.5
IV	3.8	1000	50	2.9

to isolate and characterize at the end of the experiment a new complex in which the metal binds a fumarate molecule originating from the hydrogenation of DMAD.

Results

The cyclotrimerization of DMAD was carried out in cyclohexane solution by adding catalytic amounts of **II**. In most experiments, the initial ratio monomer/catalyst was *ca.*1000 and the time dependence of [DMAD] was followed by GLC. The plots of ln[DMAD] *vs* time obtained at 25, 34, 42, and 50 °C (catalyst concentration [**II**] = 3.8×10^{-4} M) are shown in Figure 1. It must be mentioned that the same reaction catalyzed by (cyclopentadienyl)RhL_2 complexes requires more drastic conditions, *viz.* several hours in boiling toluene.[1a]

After an induction period that decreases with increasing temperature, the plots of ln[DMAD] *vs* time become linear up to almost quantitative conversion of the monomer; the calculated first-order rate constants, k_{obsd}, at four different temperatures ranging from 25 to 50 °C are listed in Table 1. It is important to emphasize the stepwise shape of the curve at 25 °C: this could be indicative of a reaction pathway consisting of at least two slow steps. Such a stepwise shape of the curve becomes much less evident at higher temperatures.

The effect of the concentration of the catalyst on k_{obsd} was investigated at 50 °C; the calculated k_{obsd} values are linearly dependent upon [**II**] and are reported in Table 1.

After complete consumption of the monomer and removal of solvent and of the trimer hexacarbomethoxybenzene, a mixture of organometallic complexes, still showing catalytic activity, was recovered and characterized by ^{1}H NMR spectroscopy, making use of the Ind* signals. The resonances of Ind* occurring at δ 2.0−2.7 ppm are well-separated from the signals due to DMAD and the trimer, which enables the analysis of the complexes in the presence of some amounts of these compounds. The spectra of the precursor **II** (spectrum A) and of the organometallic residue (spectrum B) are shown in Figure 2. Spectrum B reveals that only two species are present in the mixture in the ratio of *ca.* 1/3, *viz.*, the precursor **II** and a new Rh−indenyl species whose spectral pattern consists of one doublet at δ 2.04, likely due to the methyl protons in position 2 (J_{Rh-H} = 2.1 Hz), and of six singlets.

To determine the structure of the new species, the residue was purified by TLC; this enabled the separation of **II** from the unknown species, the ^{1}H NMR spectrum of which is shown in Figure 3. In addition to the seven resonances mentioned above, the spectrum shows a sharp signal at δ 3.58 (6H) due to two methoxy groups and a broad signal at δ *ca.* 3.76 (2H). At 183 K the sharp singlet splits into two singlets at δ 3.65 and 3.63, and the broad signal is replaced by an AB pattern (δ 3.83 and 3.85, J_{AB} = 9.9 Hz) (see inset in Figure 3). A careful examination of this part of the spectrum reveals the existence of a different coupling interaction between ^{103}Rh and the two AB protons, this interaction being detectable only for the low-field component (J_{Rh-H} = 2.1 Hz). In the IR spectrum, besides two strong absorption bands at 1945 and 1870 cm^{-1} due to the Cr-$(CO)_3$ group, only one band was detected at 2018 cm^{-1}, *i.e.*, in the region of the stretching absorption modes typical of rhodium-bonded CO's, so that only one CO group appears to be bonded to the metal. From these results we argued that the above-mentioned NMR spectral pattern is due to the presence of a *trans* olefinic ligand π-coordinated to rhodium.

Crystals of this compound suitable for X-ray analysis were obtained by slow evaporation of concentrated 1/10 (v/v) CH_2Cl_2−pentane mixtures (data collection and structure refinement parameters are collected in Table 2). A view of the molecular structure giving the atom-numbering scheme is shown in Figure 4; atom labeling and selected bond distances and angles are listed in Table 3. It appears that the *trans*-[$Cr(CO)_3$−Ind*−RhL_2] structure is preserved in the complex; however, one of the carbonyls of the precursor is replaced by a molecule of dimethyl fumarate, giving *trans*-[$Cr(CO)_3$−Ind*−Rh(CO)(FADE)] (**III**; FADE = fumaric acid dimethyl ester), an olefin that must originate from hydrogenation of a DMAD molecule. The presence of a molecule of *trans*-alkene as an ancillary ligand at the rhodium atom makes the complex intrinsically chiral; thus, the seven methyl groups of the indenyl ligand are diastereotopic and magnetically nonequivalent, as indicated by the ^{1}H and ^{13}C NMR spectra (see Experimental Section).

Complex **III** was prepared independently by easy replacement of one of the carbonyls of **II** by FADE in CH_2Cl_2 at 35 °C. Following the same procedure, we synthesized the complex *trans*-[$Cr(CO)_3$−Ind*−Rh(CO)-(MADE)] (**IV**; MADE = maleic acid dimethyl ester) by using excess MADE. The X-ray structure of this complex is reported in Figure 5; atom labeling and the

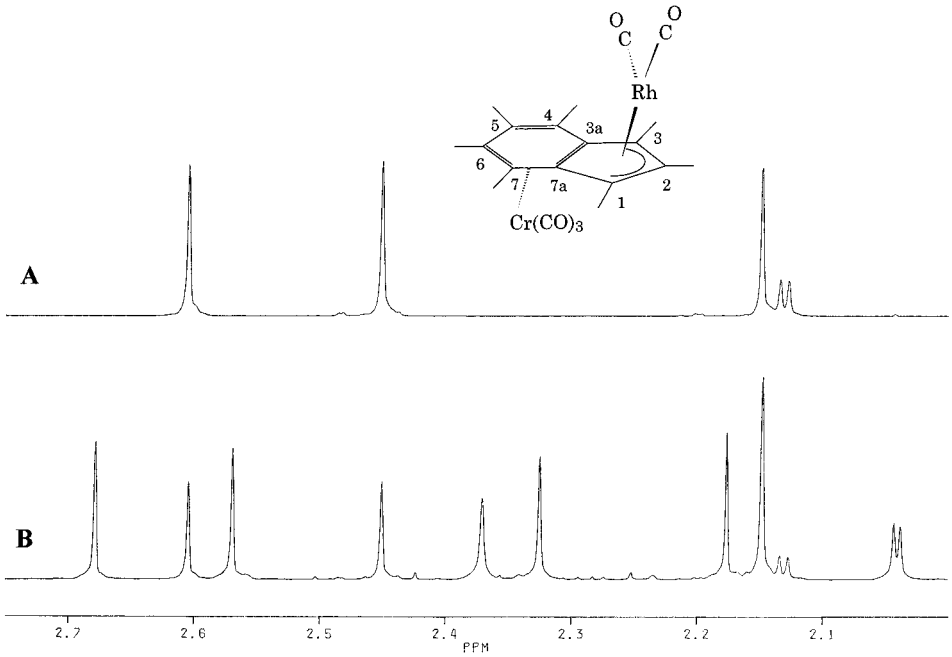

Figure 2. ^{1}H NMR spectrum (ν_0 400.133 MHz) of (A) *trans*-[Cr(CO)$_3$−Ind*−Rh(CO)$_2$] (**II**) and (B) the organometallic residue isolated at the end of the catalytic runs (T = 298 K, solvent, CD_2Cl_2; δ values are given in ppm from Me_4Si as the internal standard.

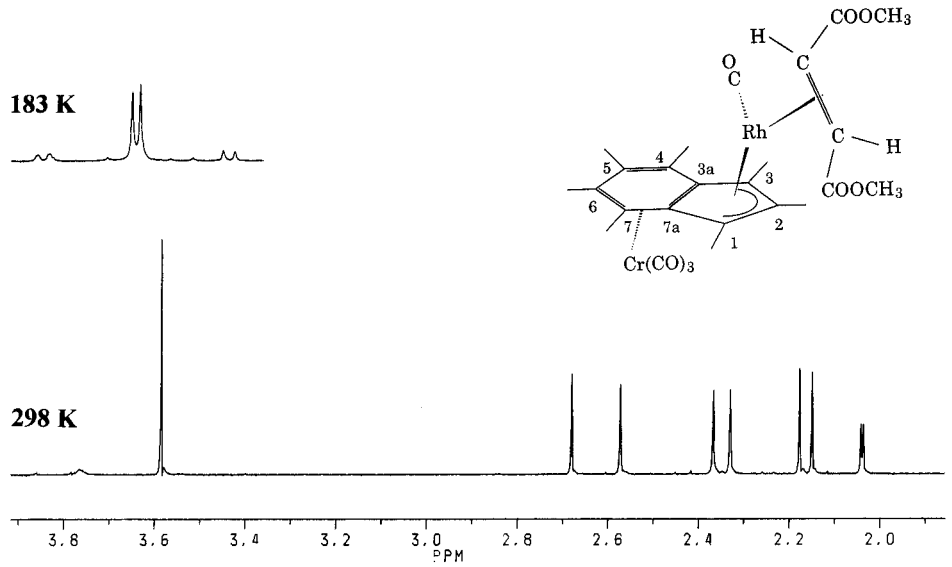

Figure 3. ^{1}H NMR spectrum (ν_0 400.133 MHz) of **III** (T = 298 K, solvent CD_2Cl_2). The inset shows the spectrum of the FADE subunit at 183 K.

most relevant bond lengths and angles are listed in Table 3. In this case, the π-coordination of a *cis*-olefin at rhodium does not introduce any asymmetry in the molecule, which, therefore, is not chiral. This is confirmed by the ^{1}H and ^{13}C NMR spectra, which show the pattern characteristic of a heptamethylindenyl skeleton where the nuclei in the 1-, 4-, and 5-positions are equivalent to those in the 3-, 7-, and 6-positions, respectively (see Experimental Section).

Both complexes **III** and **IV** exhibit catalytic activity in the cyclotrimerization reaction comparable to that found for precursor **II**, as can be seen from the values of k_{obsd}'s reported in Table 1. However, the plots of ln-[DMAD] *vs* time indicate that the induction period is substantially shorter in the runs carried out with **III** and **IV** instead of **II** (a comparison of the three complexes is shown in Figure 6).

Once the spectroscopic characteristics of complexes **III** and **IV** were known, it became possible to investigate the fate of precursor **II** during the cyclotrimerization reaction. Trimerization, carried out at 50 °C, was interrupted at different times varying between 1 and 30 min, corresponding to conversions from 6 to 95%. The organometallic components of the mixture were then separated from the organic substrates, and the analysis of the ^{1}H NMR spectra in the methyl proton region (*i.e.* that corresponding to the Ind* spectrum) leads to the following conclusions.

(i) The signals of the catalyst precursor **II** are absent even in the first spectrum recorded at t = 1 min. They reappear, together with those of complex **III**, only in the spectrum of the reaction mixture sampled after *ca.* 2 h ($t = \infty$).

(ii) Complex **III** is present, to a minor extent, even at

Table 2. Data Collection and Structure Refinement Parameters for the Complexes *trans*-[Cr(CO)$_3$−Ind*−Rh(CO)(FADE)], III, and *trans*-[Cr(CO)$_3$−Ind*−Rh(CO)(MADE)] IV

	III	IV
formula	$RhCrO_8C_{26}H_{29}$	
M_r	624.41	
space group	$P2_1/n$	$P\bar{1}$
a/Å	18.060(2)	13.821(2)
b/Å	7.987(1)	12.825(1)
c/Å	18.560(2)	7.687(1)
α/deg	90	102.5(1)
β/deg	98.6(2)	100.0(1)
γ/deg	90	83.8(1)
V/Å^3	2647.1	1306.5
Z	4	2
cryst dimens/mm	0.2 × 0.20 × 0.3	0.3 × 0.25 × 0.25
D_c, g cm^{-3}	1.57	1.59
μ/cm^{-1}	11.22	11.37
T, K	298	
radiation (λ (Å))	graphite-monochromated Mo Kα (λ = 0.7107)	
takeoff angle/deg	3	
scan speed/(deg min^{-1})	2.0 in 2θ scan mode	
scan width/deg	1.2	
2θ range/deg	2.0 ≤ 2θ ≤ 45	
no. of unique reflections ($F_o^2 > 2\sigma(F_o^2)$)	3386	3884
R (on F_o)	0.056	0.044
R_w	0.056	0.047
GOF	1.07	0.93

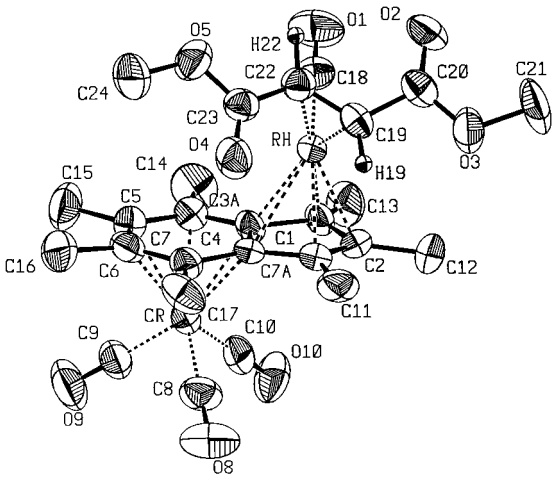

Figure 4. ORTEP[20] drawing of *trans*-[Cr(CO)$_3$−Ind*−Rh-(CO)(FADE)] (**III**). Thermal ellipsoids are shown at the 50% probability level.

the beginning of the reaction and becomes the main component of the organometallic residue at $t = \infty$.

(iii) The spectrum of the mixture sampled at $t = 1$ min shows that the main component is a new species whose signals (δ 2.46 (6H), 2.22 (6H), 2.11 (3H) ($J_{Rh-H} \cong 2$ Hz), 1.97 (6H)) are indicative of a symmetric heptamethylindenyl framework, very likely due to the monosubstituted *trans*-[Cr(CO)$_3$−Ind*−Rh(CO)(DMAD)] complex **V**, bearing an alkyne ligand, in agreement with analogous systems described in the literature.[5] The resonances corresponding to this species are observed, albeit in decreasing intensity, in all the spectra recorded at different times and disappear only at $t = \infty$.

(iv) The signals corresponding to complex **IV** were never observed.

(v) As mentioned above, examination of the ^{1}H NMR spectrum at $t = \infty$ indicates the presence of only complexes **II** and **III**, in the ratio of *ca.* 1/3.

(5) (a) Wakatsuky, Y.; Yamazaki, H. *J. Organomet. Chem.* **1974**, *64*, 393. (b) McAlister, D. R.; Berkau, J. E.; Bergman, R. G. *J. Am. Chem. Soc.* **1977**, *99*, 1666.

Table 3. Selected Bond Lengths (Å), Bond Angles (deg), and Torsion Angles (deg) for the Complexes *trans*-[Cr(CO)$_3$−Ind*−Rh(CO)(FADE)] (III) and *trans*-[Cr(CO)$_3$−Ind*−Rh(CO)(MADE)] (IV)

	III	IV
Bond Lengths		
Rh−C1	2.259(8)	2.217(6)
Rh−C2	2.205(8)	2.243(5)
Rh−C3	2.208(8)	2.228(5)
Rh−C3a	2.2413(8)	2.367(5)
Rh−C7a	2.452(8)	2.370(5)
Cr−C3a	2.286(8)	2.295(5)
Cr−C4	2.273(9)	2.251(6)
Cr−C5	2.240(9)	2.225(7)
Cr−C6	2.243(9)	2.223(6)
Cr−C7	2.249(8)	2.254(6)
Cr−C7a	2.312(9)	2.296(5)
C1−C2	1.43(1)	1.430(7)
C2−C3	1.42(1)	1.407(8)
C3−C3a	1.48(1)	1.465(7)
C3a−C7a	1.50(1)	1.455(7)
C7a−C1	1.44(1)	1.461(7)
C3a−C4	1.43(1)	1.435(8)
C4−C5	1.41(1)	1.435(8)
C5−C6	1.45(1)	1.396(8)
C6−C7	1.42(1)	1.43(1)
C7−C7a	1.43(1)	1.412(9)
C22−C19	1.38(1)	1.439(8)
C23−O4	1.22(1)	1.184(6)
C20−O2	1.22(1)	1.198(7)
Bond Angles		
C19−C22−C23	121.9(8)	124.2(5)
C22−C23−O4	125.6(8)	125.7(6)
C22−C19−C20	122.2(8)	122.5(6)
C19−C20−O2	124.9(8)	123.0(6)
Torsion Angles[a]		
C20−C19−C22−C23	−155	−7
C22−C23−O5−C24	178	178
C19−C20−O3−C21	179	181
C10−Cr−M−C3a	−13	33
C9−Cr−M−C5	−15	28
C8−Cr−M−C7	−16	27

[a] M represents the center of the benzene ring.

The same NMR investigation performed using complex **III** as catalyst precursor showed exactly the same trend as reported above for complex **II**. In the first spectrum, corresponding to $t = 1$ min, **V** is present as

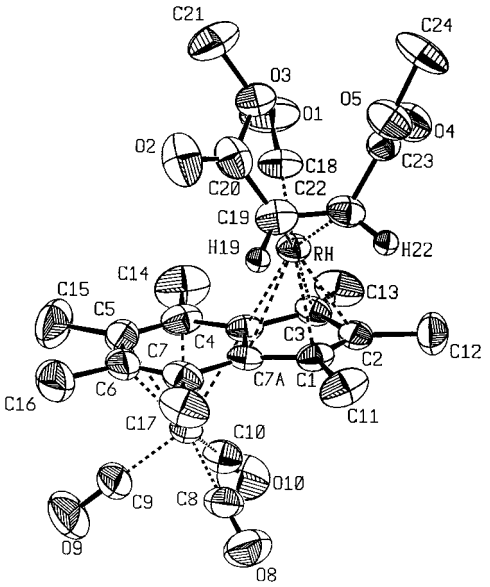

Figure 5. ORTEP[20] drawing of *trans*-[Cr(CO)$_3$−Ind*−Rh(CO)(MADE)] (**IV**). Thermal ellipsoids are shown at the 50% probability level.

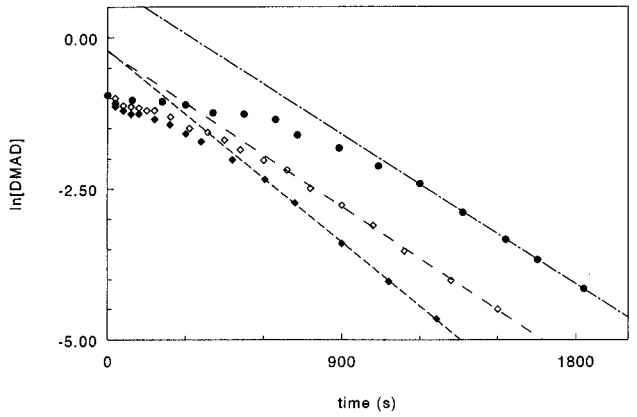

Figure 6. Plots of ln[DMAD] *vs* time for the cyclotrimerization reaction of DMAD catalyzed by **III** (◆), **IV** (◇), and **II** (●) (solvent cyclohexane, T = 50 °C, $[DMAD]_0$ = 0.387 M, $[DMAD]_0/[cat.]$ = 1000).

the main component of the mixture; the spectrum does not change substantially during the reaction, and at $t = \infty$ the organometallic residue has the same composition as found using **II** as catalyst. It is striking that after the monomer is consumed, most of complex **III** is re-formed along with **II**, in which both ancillary ligands at rhodium are carbonyls. Thus, the structure of the catalytic precursor is preserved when the cyclotrimerization reaction is over and a new crop of monomer can be cyclotrimerized to benzene derivatives.

Description of the Structures of *trans*-[Cr(CO)$_3$−Ind*−Rh(CO)(FADE)] (III) and *trans*-[Cr(CO)$_3$−Ind*−Rh(CO)(MADE)] (IV). A comparison between the structural features of complexes **III** and **IV** may be instructive. In complex **III** the Cr(CO)$_3$ tripod is bonded to the six-membered ring of the heptamethylindenyl ligand in a conformation halfway between staggered and eclipsed (see Figure 4 and Table 3); this is explained only in terms of crystal-packing effects, since there is no apparent intramolecular reason. The chromium atom shows a slight slippage (*ca.* 0.05−0.06 Å) toward the C5−C6 bond and seems to retain the usual almost undistorted η^6 bonding mode; no hinge angle is observed for the benzene ring. In contrast, the rhodium atom is coordinated to the five-membered ring in a rather distorted η^5 mode, as evidenced by the hinge angle (*ca.* 8−9°) between the planes [C1,C2,C3] and [C1,C3,C3a,-C4,C7,C7a], with C2 out of the indenyl plane by *ca.* 0.12 Å to the same side of chromium. A comparison with the molecular structure of the precursor complex **II**[3b] reveals that these and other described distortions arise from intramolecular constraints due to the olefinic ligand. The olefin is coordinated to rhodium through one of the two prochiral faces of its *trans*-substituted double bond; the coordination geometry about rhodium is rather distorted, as shown by (i) the angle between the planes [C1,C2,C3] and the line through C19−C22 (*ca.* 25° as opposed to their being parallel in an undistorted geometry)[6] and (ii) the quite different distances Rh−C19 (2.13 Å) and Rh−C22 (2.19 Å). These features are imposed by the need to relieve the nonbonded intramolecular interactions mainly between O4···C$_7$ (3.30 Å apart) and O4···C17 (3.08 Å apart). These interactions are counterbalanced by short contacts in the range of 3.4−3.5 Å between O3, C2, and C12, showing that they cannot be relieved through a further rotation of the olefinic ligand about the Rh−olefin axis. A narrower bond angle olefin−Rh−CO would be useful for this purpose, but it is precluded by short contacts with the CO group; the wider angle Cp−Rh−olefin is likely inhibited by severe geometrical requirements. The torsion angle about C19−C22 is *ca.* 155°, and the bond distance C19−C22 is lengthened to 1.38 Å. These last parameters cannot be explained only in terms of rhodium-to-olefin back-donation, though it is certainly cooperative in this structure. This behavior is quite common for *trans* olefinic groups coordinated through a $\sigma-\pi$ bond to metals and has been observed in other complexes with the same fumarate ligand.[7] The other geometrical parameters of the molecule are in the norm. It should be mentioned that the observed molecular conformation is likely to be the one of minimum internal energy. The only other reliable conformer obtained from an idealized rotation of 180° about the Rh−Cp axis, with the *trans* olefin in the same configuration, would be strongly inhibited by short contact distances from the Ind* ligand methyls. Actually, this can be easily inspected with suitable models if we assume that the C19−C22 bond must maintain almost the same or a less distorted orientation as that found in this structure, which is imposed by geometrical coordination requirements.

Among the organometallic complexes that are present at $t = \infty$, not even the smallest amount of the *cis* derivative (complex **IV**) was detected, probably due to the stereospecificity of the hydrogenation mechanism of the alkyne. In the case of a *cis* configuration of the olefin the only configuration to be expected is the one bearing the ester groups toward the outer side of the molecule. In fact, the conformation shown in the solid state (see Figure 5) by complex **IV**, obtained by direct displacement of CO in **II**, corresponds to this expectation. As a whole, the structure of **IV**, if compared with that of **III**, shows a substantially less distorted molec-

(6) Bonifaci, C.; Ceccon, A.; Gambaro, A.; Ganis, P.; Santi, S.; Valle, G.; Venzo, A. *J. Organomet. Chem.* **1995**, *492*, 35 and references quoted therein.

(7) Albano, V. G.; Castellari, C.; Monari, M.; De Felice, V.; Panunzi, A.; Ruffo, F. *Organometallics* **1995**, *14*, 4213.

ular geometry: (i) the five-membered ring is almost exactly planar, having an hinge angle of only 2−3° between the planes [C1,C2,C3] and [C1,C3,C3a,C4,C7,-C7a]; (ii) the coordination geometry about rhodium is almost undistorted, as substantiated by the coplanarity of the line through bond C19−C22 and the plane [C1,-C2,C3]; (iii) the bond C3a−C7a (1.45 Å) is shorter than that found in complex **III** (1.50 Å) (but still raises the same question about the hapticities of the metals); (iv) no severe intramolecular nonbonding interactions are observed. Yet, the olefinic double bond of the maleate ligand is elongated as expected and found in similar coordinated systems.[8] These data prove that the geometrical distortions observed in **III** are mainly controlled by the conformation of the olefinic ligand.

Discussion

The mechanism of cyclotrimerization of alkynes to benzenes catalyzed by low-valent transition-metal complexes is already known and generally accepted.[1b,9] According to this mechanism, in complexes such as $CpML_2$ the initial step is the sequential substitution of the two ligands to give CpML(alkyne) and $CpM(alkyne)_2$. On reaction of the dialkyne complex with DMAD, metallacyclic intermediates are formed. While the present investigation does not furnish further information on the steps of the catalytic cycle, it sheds some light on the two initial steps involving substitution of the ancillary ligands at rhodium. Moreover, the experiment carried out with complex **III** as catalyst precursor suggests a reaction path in which none of the original ancillary ligands of the precursor remains bound to the rhodium atom throughout the catalytic cycle. Finally, isolation of complex **III** at the end of the cyclotrimerization is indicative of the existence of an intermolecular C−H bond activation of cyclohexane as a source of hydrogen.

Monosubstitution of one carbon monoxide in precursor **II** by one alkyne molecule is a very fast step, as shown by the complete disappearance of the signals characteristic of **II** in the ^{1}H NMR spectrum recorded after only 1 min from the start of the reaction. Substitution of the fumarate ligand when complex **III** is used as precursor must also occur rapidly, since identical ^{1}H NMR spectra are recorded during the induction period in both cases. It has been shown that substitution of the ancillary ligands at rhodium in indenyl complexes is greatly accelerated in comparison to the cyclopentadienyl analogues,[2] and a further strong acceleration is observed when the benzene ring of the indenyl frame is coordinated to a $Cr(CO)_3$ moiety located *anti* with respect to rhodium.[3a,10] Thus, the signals of the main component of the organometallic mixture sampled during the induction period must belong to *trans*-[$Cr(CO)_3$−Ind*−Rh(CO)(DMAD)] (**V**). This assignment is in agreement with the symmetric pattern shown by the indenyl methyl signals in the ^{1}H NMR spectrum of these complexes; here the chemical shifts occur at slightly higher field (by *ca.* −0.2 ppm) with respect to those of complex **II** (parenthetically, cyclopentadienylcobalt complexes in which one alkyne molecule is coordinated to the metal have been isolated[5b]). As far as the very fast formation of the chiral *trans*-[$Cr(CO)_3$−Ind*−Rh(CO)-(FADE)] complex **III** is concerned, there is no question that hydrogenation of DMAD to give FADE did take place, probably within the coordination sphere of rhodium. There are several ways in which this may occur, and the attractive hypothesis of C−H bond activation of cyclohexane as a source of hydrogen will be discussed later.

It is likely that the substitution of the second CO of the monoalkyne derivative **V** is the slow step generating the active catalyst, *i.e.*, *trans*-[$Cr(CO)_3$−Ind*−Rh(DMAD)$_2$] (**VI**); this species then initiates the catalytic cycle. This hypothesis allows us to rationalize the long induction period observed in our experiments (Figure 1) and can be justified by the well-known stability of complexes such as (indenyl)Rh(CO)L, where L is a donor ligand;[2e] these are not very prone to substitution of the CO. It should be mentioned that when complex **III** (or **IV**) was used instead of **II** as catalyst precursor, comparable catalytic activities were found (see Table 1), indicating that in both cases the same active catalyst, **VI**, is operative. Moreover, since the ^{1}H NMR spectra recorded at different times are identical when one starts from either **II** or **III**, the mechanism of formation of **VI** should be quite similar in both cases. However, the markedly shorter induction period found for the reaction carried out in the presence of **III** (or **IV**) suggests that in this case the active catalyst, **VI**, may be formed more readily *via* an alternative ligand substitution pathway, competitive with the former (see Scheme 1).

The residue recovered at the end of the cyclotrimerization reaction is largely made up of a mixture of complexes **II** and **III** in a 1/3 ratio; no detectable decomposition products of the organometallic species are found. The same results were obtained by using **III** as catalyst precursor; therefore, in order to justify the formation of the bicarbonylated complex, both ancillary ligands of **III** must undergo the exchange reaction. Complex **III** represents the main component of the final organometallic mixture: it accumulates when DMAD is lacking but is consumed by a substitution reaction to give the "true" catalyst when DMAD is in excess. Therefore, its concentration is very low and almost constant throughout the reaction.

From the detailed mechanistic analysis of the cyclotrimerization reaction reported here and from the previously suggested[1b,9] mechanistic hypothesis for the same reaction, a complete pathway for the cyclotrimerization of DMAD catalyzed by **II** is sketched in Scheme 1.

Finally, an interesting question is whether hydrogenation of the alkyne ester to give the fumarate took place *via* an intermolecular C−H bond activation of cyclohexane as a source of hydrogen, an intramolecular C−H activation of Ind* methyls, or some unknown hydrogenation pathway. (We checked carefully whether FADE or other hydrogen-donating impurities were present in DMAD as well as in the purified cyclohexane. Spectroscopic and MS-GLC spectrometric analyses have ruled out the presence of these compounds). Indeed, the C−H activation reaction of alkane solvents by organo-

(8) (a) Ganis, P.; Pedone, C. *Ric. Sci.* **1965**, *35*, 3. (b) Ganis, P.; Dunitz, J. D. *Helv. Chim. Acta* **1967**, *50*, 2379 and references quoted therein.

(9) Parshall, G. W.; Ittel, S. D. *The Application and Chemistry of Catalysis by Soluble Transition Metal Complexes*, 2nd ed.; Wiley: New York, 1993; pp 208−212.

(10) Bonifaci, C.; Carta, G.; Ceccon, A.; Gambaro, A.; Santi, S.; Venzo, A. *Organometallics* **1996**, *15*, 1630.

Scheme 1. Proposed Mechanism for the Cyclotrimerization Reaction of DMAD Catalyzed by *trans*-[Cr(CO)$_3$−Ind*−Rh(CO)$_2$

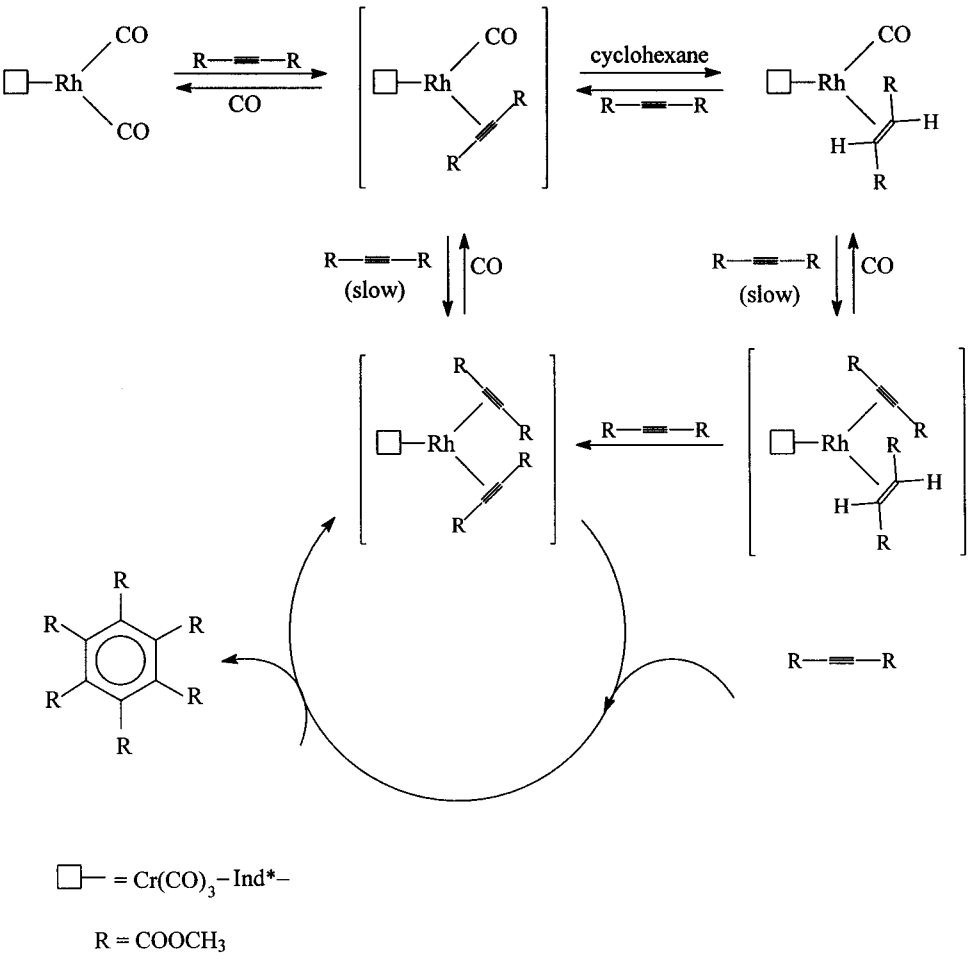

metallic compounds, most likely rhodium and iridium pentamethylcyclopentadienyl complexes, has been extensively studied.[11] These metal-based homogeneous processes typically require photochemistry or relatively high temperatures in order to produce the reactive intermediates believed to be responsible for the oxidative addition of the hydrocarbon. Recently, Bergman[12] reported an unusual example of alkane activation by the iridium complex $[(Cp^*)Ir(PMe_3)(CH_3)(CH_2Cl_2)]^+$ even at low temperature, where the reactive $[(Cp^*)Ir(PMe_3)(CH_3)]^+$ fragment is easily formed by loss of the CH_2Cl_2 ligand. One of the requirements for a two-electron oxidation of the metal leading to a hydrido(alkyl)metal complex is, in fact, a coordinative unsaturation enabling access to the metal valence orbitals. The presence in the precursor of very labile ancillary ligands is a decisive factor for the thermal formation of the unsaturated fragment. Electronic unsaturation necessary for accommodation of the C−H electrons and an accessible $n + 2$ oxidation state of the metal are also of importance for the occurrence of the process under mild conditions. All these requirements are met in the complexes of structure *trans*-[Cr(CO)$_3$−Ind*−RhL$_2$]. In fact, the coordination of the benzene ring with Cr(CO)$_3$ associated with the flexibility of the indenyl ligand introduces significant modifications of the electronic distribution of the complex even in the ground state. On the basis of spectroscopic[13] and kinetic[3a,10] data we suggested that the ground state of these bimetallic complexes is represented in solution by a fast equilibrium between the haptomers **1** and **2**. In **1**, rhodium is

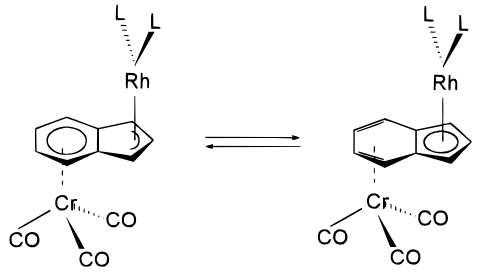

(**1**) (**2**)

coordinatively unsaturated and is prone to easily receive a new ligand in its coordination sphere; moreover, electronic unsaturation at rhodium is provided by the strong electron-withdrawing effect of the tricarbonylchromium group. Hence, if the coordination mode of rhodium in these bimetallic compounds is shifted toward an increased allyl−ene character in bonding to the five-membered ring, favored by aromatization of the benzene

(11) (a) Crabtree, R. H. *Chem. Rev.* **1985**, *85*, 245. (b) Schultz, R. H.; Bengali, A. A.; Tauber, M. J.; Weiller, B. H.; Wasserman, E. P.; Kyle, K. R.; Bradley Moore, C.; Bergman, R. G. *J. Am. Chem. Soc.* **1994**, *116*, 7369. (c) Arndtsen, B. A.; Bergman, R. G.; Mobley, T. A.; Peterson, T. H. *Acc. Chem. Res.* **1995**, *28*, 154. (d) Paneque, M.; Taboada, S.; Carmona, E. *Organometallics* **1996**, *15*, 2678.

(12) Arndtsen, B. A.; Bergman, R. G. *Science* **1995**, *270*, 1970.

(13) Ceccon, A.; Elsevier, C. J.; Ernsting, J. M.; Gambaro, A.; Santi, S.; Venzo, A. *Inorg. Chim. Acta* **1993**, *204*, 15.

ring,[14] substitution of ligand L and attack by the C−H bond electrons should be strongly facilitated. As a matter of fact, we have shown that the rate of substitution of CO's by olefins (COD and NBD) increases by a factor of 2×10^3 if the benzene ring of the indenyl ligand is complexed in a transoid mode to $Cr(CO)_3$.[10] Thus, fast attack by the C−H bond of cyclohexane may be competitive with substitution of CO by the alkyne monomer, forming an alkyl hydride intermediate followed by hydrogenation of the coordinated alkyne to FADE. Indeed, as recent results have shown,[15] C−H bond activation is a very fast process with a free energy of activation $\Delta G^{\ddagger} = 4.5$ kcal/mol for cyclohexane. If the activation energy for substitution of the two CO's by DMAD to form the true catalyst is similar to that measured for the same substitution reaction with COD, *i.e.*, *ca.* 10 kcal/mol, the oxidative-addition reaction should be even faster than the formation of the true catalyst. Actually, the spectroscopic analysis has shown that the FADE complex is already present in solution at the beginning of the reaction during the induction period.

It should be pointed out that our interpretation of the hydrogenation of DMAD based on C−H activation of cyclohexane requires more accurate experimental evidence. However, C−H bond activation by rhodium indenyl complexes under mild conditions is not unprecedented. In the trimerization of but-2-yne catalyzed by Ind−Rh(ethylene)$_2$ at room temperature,[16a] formation of bridged dinuclear vinyl complexes of rhodium was explained by assuming cleavage of an ethylenic carbon−hydrogen bond, resulting in the formation of a rhodium-vinyl bond. The same indenyl complex is a catalyst for intermolecular hydroacylation, *viz.*, the addition of aldehydes to alkenes.[16b] Even in this case, the structure of the catalyst precursor is characterized by the presence of the flexible indenyl ligand and of easily displaceable ancillary ligands, *i.e.*, ethylene. It seems, therefore, that *trans*-[Cr(CO)$_3$−Ind*−RhL$_2$] complexes are structurally promising systems for activation of C−H bonds under mild thermal conditions. Perhaps bimetallic Ind* complexes of Cr(0) and Ir(I) will be even more convenient for favorable results in this field, and our experimental investigation is now directed toward obtaining more information on C−H bond activation by these complexes.

Experimental Section

NMR spectra were measured on a Bruker AM400 spectrometer operating in the FT mode at 400.133 and 100.614 MHz for ^{1}H and ^{13}C, respectively. Chemical shifts are given from Me_4Si as internal standard. The ^{13}C peak assignment was based on selective proton decoupling experiments and partially relaxed spectra. The proton assignments were based on ^{1}H-{^{1}H} NOE measurements: the usual procedure for gated experiments was modified,[17] and the selected multiplet was saturated by a 10 s cyclic perturbation of all lines with a 42 dB attenuation of a nominal 0.2 W decoupling power.

IR spectra were run as CH_2Cl_2 solutions (optical length 0.2 mm, CaF_2 windows) on a Perkin-Elmer 580B spectrophotometer equipped with a Perkin-Elmer 3600 data acquisition system. The 70 eV EI mass spectra were recorded on a VG MicroMass-16 spectrometer. GLC analyses were obtained on a Varian Model 3700 gas−liquid chromatograph equipped with a Shimadzu CR-5A signal integrator.

All reactions were carried out in oxygen-free solutions under a blanket of purified argon. Solvents were purified according to standard procedures,[18] distilled, and purged with argon before use. Commercial grade DMAD (Aldrich, 99%) was distilled under reduced pressure just before use and checked for traces of FADE and other hydrogen-donating impurities by MS−GLC (the measured purity was ≥99.95%). Syntheses and characterization of *trans*-[Cr(CO)$_3$−Ind*−Rh(COD)] (**I**) and *trans*-[Cr(CO)$_3$−Ind*−Rh(CO)$_2$] (**II**) have previously been reported.[3b]

***trans*-[Cr(CO)$_3$(heptamethylindenyl)Rh(CO)(FADE)] (III).** A 10^{-2} M solution of **II** in CH_2Cl_2 was treated with a 10-fold excess of FADE at 35 °C for 1 h, at which point TLC analysis showed complete disappearance of **II**. The solvent was removed by an argon stream and the residue washed with pentane, affording a quantitative yield of **III**. Mp: 155 ° C dec. Anal. Calcd for $C_{26}H_{29}CrO_8Rh$: C, 50.01; H, 4.68. Found: C, 50.35; H, 4.87. MS (*m/z*): 624 (M^+, 6.9%), 596 (M^+ − CO, 1.4), 568 (M^+ − 2CO, 5.5), 540 (M^+ − 3CO, 15.9), 512 (M^+ − 4CO, 10.3), 480 (M^+ − FADE, 2.8), 460 (M^+ − [Cr, (4CO)], 18.6), 452 (M^+ − (FADE, CO), 2.0), 424 (M^+ − [FADE, 2(CO)], 13.1), 396 (M^+ − [FADE, 3(CO)], 34.5), 368 (M^+ − [FADE, 4(CO)], 7.6), 316 (M^+ − [FADE, Cr, 4(CO)], 77.9), 265 (M^+ − [FADE, Cr, Rh, 4(CO)], 6.9), 113 (Rh^+, 100), 52 (Cr^+, 46.9). Spectroscopic data: IR ν_{max} (CH_2Cl_2) 2018 m (Rh−C≡O), 1946 vs and 1868 vs (Cr−C≡O), 1707 m cm^{-1} (FADE ester C=O); ^{1}H NMR (CD_2Cl_2, $T = 298$ K) δ 3.76 (broad s, 2H, FADE olefinic protons), 3.583 (s, 6H, FADE methyl protons), 2.678 (s, 3H, 4-CH_3), 2.569 (s, 3H, 7-CH_3), 2.370 (s, 3H, 3-CH_3), 2.324 (s, 3H, 1-CH_3), 2.176 (s, 3H, 5-CH_3), 2.147 (s, 3H, 6-CH_3), and 2.041 (d, 3H, $J(^{103}Rh-H) = 2.1$ Hz, 2-CH_3); ^{1}H NMR (CD_2Cl_2, $T = 183$ K) δ 3.847 (dd, 1H, $J_{AB} = 9.9$ Hz, $J(^{103}Rh-H)$ *ca.* 2.1 Hz, one olefinic FADE proton), 3.438 (broad d, 1H, $J_{AB} = 9.9$ Hz, the other FADE olefinic proton), 3.651 and 3.633 (two s, 3H each, FADE CH_3 protons), 2.704 (s, 3H, 4-CH_3), 2.556 (s, 3H, 7-CH_3), 2.509 (s, 3H, 3-CH_3), 2.264 (s, 3H, 1-CH_3), 2.231 (s, 3H, 5-CH_3), 2.179 (s, 3H, 6-CH_3), 2.139 (broad, 3H, 2-CH_3); ^{13}C NMR (CD_2Cl_2, $T = 298$ K) δ 234.50 (Cr−*C*≡O), 189.13 ($J(^{103}Rh-^{13}C) = 89.7$ Hz, Rh−*C*≡O), 173.22 (FADE *C*(O)O), 120.20 ($J(^{103}Rh-^{13}C) = 6.0$ Hz, C2), 107.14 and 106.53 (C5 and C6), 105.3 (broad, C3a and C7a), 99.50 and 97.21 (C7 and C4), 91.94 ($J(^{103}Rh-^{13}C) = 3.3$ Hz, C1), 91.57 ($J(^{103}Rh-^{13}C) = 4.5$ Hz, C3), 51.95 (FADE C(O)O*C*H$_3$), 51.0 (broad, FADE olefinic carbons), 17.81 (7-CH_3), 16.98 (5-CH_3 and 4-CH_3), 16.79 (6-CH_3), 14.15 (3-CH_3), 13.53 (1-CH_3), 11.87 (2-CH_3).

***trans*-[Cr(CO)$_3$(heptamethylindenyl)Rh(CO)-(MADE)] (IV).** This complex was obtained in quantitative yield by reacting a 10^{-2} M solution of **II** in CH_2Cl_2 for 2 h at 35 °C with excess MADE (50 equiv). The solvent and most of the unreacted MADE were pumped off, and the residue was washed with pentane. Mp: 150 °C dec. Anal. Calcd for $C_{26}H_{29}CrO_8Rh$: C, 50.01; H, 4.68. Found: C, 50.18; H, 4.57. MS (*m/z*): 624 (M^+). Spectroscopic data: IR ν_{max} (CH_2Cl_2) 2022 m (Rh−C≡O), 1946 vs and 1868 vs (Cr−C≡O), 1710 m cm^{-1} (MADE ester C=O); ^{1}H NMR (CD_2Cl_2, $T = 298$ K) δ 3.556 (s, 6H, MADE methyl protons), 3.492 (d, 2H, $J(^{103}Rh-H) = 2.5$ Hz, MADE olefinic protons), 2.664 (s, 6H, 4,7-CH_3), 2.205 (s, 6H, 1,3-CH_3), 2.176 (s, 6H, 5,6-CH_3), and 2.025 (d, 3H, $J(^{103}Rh-H) = 2.1$ Hz, 2-CH_3); ^{1}H NMR (CD_2Cl_2, $T = 193$ K) δ = 3.689 and 3.461 (two d, 1H each, $J_{AB} = 9.1$ Hz, olefinic MADE protons), 3.465 and 3.527 (two s, 3H each, CH_3 MADE protons), 2.758 and 2.618 (two s, 3H each, 4-CH_3 and 7-CH_3), 2.608 and

(14) Kündig, E. P.; Perret, C.; Spichiger, S. *J. Organomet. Chem.* **1985**, *286*, 183.
(15) (a) Wasserman, E. P.; Bradley Moore, C.; Bergman, R. G. *Science* **1992**, *255*, 315. (b) Siegbahn, P. E. M. *J. Am. Chem. Soc.* **1996**, *116*, 1487 and references therein.
(16) (a) Caddy, P.; Green, M.; Smart, L. E.; White, N. *J. Chem. Soc., Chem. Commun.* **1978**, 839. (b) Marder, T. B.; Roe, D. C.; Milstein, D. *Organometallics* **1988**, *7*, 1451.
(17) Kinns, M.; Sanders, J. K. M. *J. Magn. Reson.* **1984**, *56*, 518.
(18) Perrin, D. D.; Armageo, W. L. F. *Purification of Laboratory Chemicals*, 3rd ed.; Pergamon Press: Oxford, U.K., 1988.

1.830 (2s, 3H each, 1-CH_3 and 3-CH_3), 2.199 and 2.178 (2s, 3H each, 5-CH_3 and 6-CH_3), 2.044 (broad s, 3H, 2-CH_3); ^{13}C NMR (CD_2Cl_2, T = 298 K) δ 234.55 (Cr−*C*≡O), 189.01 ($J(^{103}Rh-^{13}C)$ = 90.2 Hz, Rh−*C*≡O), 171.52 (MADE *C*(O)O), 121.21 ($J(^{103}Rh-^{13}C)$ = 5.9 Hz, C2), 106.54 (C5,6), 107.13 (broad, C3a and C7a), 98.41 (C4,7), 88.93 (C1,3), 52.18 (MADE C(O)O*C*H_3), 51.6 (broad, MADE olefinic carbons), 17.18 (4,7-CH_3), 16.87 (5,6-CH_3), 13.09 (1,3-CH_3), 11.99 ($J(^{103}Rh-^{13}C)$ *ca.* 1 Hz, 2-CH_3).

Catalytic Measurements. In a typical run, to a solution of 1 mL of the DMAD monomer in 20 mL of cyclohexane kept in a Schlenk tube at 25, 34, 42, and 50 °C a few microliters of a CH_2Cl_2 solution of the catalyst was added in order to obtain a [monomer]/[catalyst] ratio of 1000/1. Aliquots 0.1 mL were withdrawn at certain time intervals and added to 0.6 mL of a cyclohexane solution 3.15×10^{-2} M in *o*-xylene used as a chromatographic internal standard; the sample was immediately cooled to −80 °C and kept at this temperature for analysis. The variation of the monomer concentration with time was monitored by GLC ($T_{inj} = T_{det}$ = 180 °C; T_c = 150 °C, FID detector; flow, 30 mL of N_2/min; column, $^1/_8$ in. i.d. 2 m length; stationary phase, SE-30 20% on Chromosorb P). The results are reported in Figure 1. In order to follow the progress of the reaction by ^1H NMR, the solvent and unreacted monomer were pumped off at −80 °C from 2 mL of the catalysis solution; the residue was dissolved in cold CD_2Cl_2 and the spectrum recorded at −20 °C. Presaturation of the signal due to the methyl protons of the trimer was required to get a satisfactory signal-to-noise ratio for the remainder of the spectrum.

Crystallography. Crystals suitable for diffractometric analysis were obtained by slow solvent evaporation from concentrated solutions of **III** and **IV** in pentane-methylene chloride. Crystal data, intensity data collection, and processing details for **III** and **IV** are presented in Table 2. The data were obtained with a Philips PW-100 four-circle diffractometer with graphite monochromator. Intensity data were collected at 25 °C using the 2θ scan method. Two reference reflections, monitored periodically, showed no significant variation in intensity. Data were corrected for Lorentz and polarization effects, and an empirical absorption correction was applied to the intensities. The positions of Cr and Rh atoms were determined from the three-dimensional Patterson function. All the remaining atoms, including hydrogens, were located from successive Fourier maps using SHELX-76.[19] Anisotropic thermal parameters were used for all the non-hydrogen atoms. Blocked-cascade least-squares refinements converged to R = 0.056 and 0.044 for **III** and **IV**, respectively. The positional parameters and the anisotropic thermal parameters of the non-hydrogen atoms, the positional parameters of the hydrogen atoms, and full lists of bond lengths and angles are available as Supporting Information.

Acknowledgment. This work was supported in part by the CNR, Rome, through its "Centro di Studio sugli Stati Molecolari Radicalici ed Eccitati" and through its Progetto Strategico "Tecnologie Chimiche Innovative". We are indebted to Dr. L. Birladeanu, Harvard University, for stimulating discussions.

Supporting Information Available: Tables giving fractional atomic coordinates, thermal parameters, and bond lengths and angles for **III** and **IV** (10 pages). Ordering information is given on any current mast head page.

OM960901+

(19) Sheldrick, G, M. SHELX-76, Program for Crystal Structure Determination, Cambridge University, Cambridge, U.K., 1976.
(20) Johnson, C. K. ORTEP; Report ORLN-3794; Oak Ridge National Laboratory, Oak Ridge, TN, 1965.